Joint Pathology Center
Veterinary Pathology Services

WEDNESDAY SLIDE CONFERENCE
2020-2021

Conference 12

December 16, 2020

Joint Pathology Center
Silver Spring, Maryland

CASE 1: W2019 234 (4134350-00)

Signalment:
10 weeks old, female entire, mini lop, domesticated European rabbit, (*Oryctolagus cuniculus)*

History:
Two nine-week-old rabbits were purchased from a breeder. The next day the other rabbit in the group presented with progressive lethargy, inappetence, bradycardia, hypothermia, seizures, and recumbency and died shortly after. Four days later this rabbit was found dead with no clinical signs noticed and was submitted for postmortem examination.

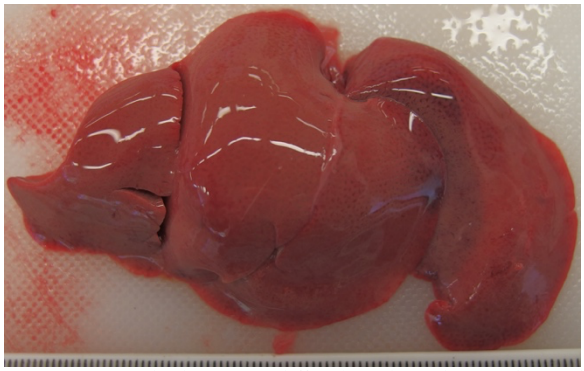

Liver, rabbit. The liver was diffusely pale with an enhanced lobular pattern and limp, friable texture. (Photo courtesy of: Department of Veterinary Medicine, The Queen's Veterinary School Hospital, University of Cambridge. Cambridge CB3 0ES, UK. https://www.vet.cam.ac.uk)

Gross Pathology:
The liver was diffusely pale brown with an enhanced lobular pattern and friable texture. The spleen was enlarged 2-fold and the edge was rounded. On both kidneys there were multifocal, poorly demarcated, up to 1 mm diameter, pin-prick, red, sub-capsular foci (petechial hemorrhages).

Laboratory results:
Fresh frozen liver was submitted for rabbit hemorrhagic disease virus (RHDV) PCR. PCR for RHDV-2 was positive and RHDV-1 was negative.

Microscopic description:
There is diffuse necrosis of periportal to midzonal hepatocytes, characterized predominantly by hypereosinophilic hepatocytes with faded nuclei (karyolysis) and retained cord architecture (coagulative necrosis). There are hepatocytes, which are multifocally dissociated from hepatic cords, that exhibit fragmented cytoplasm and karyorrhexis or pyknosis and are sometimes admixed with erythrocytes (lytic necrosis). Necrotic periportal hepatocytes infrequently exhibit numerous, variably sized, dark basophilic, cytoplasmic granules that stain positively with Von Kossa stain (calcification). There are small numbers of either individual or clustered heterophils scattered within necrotic areas. Portal

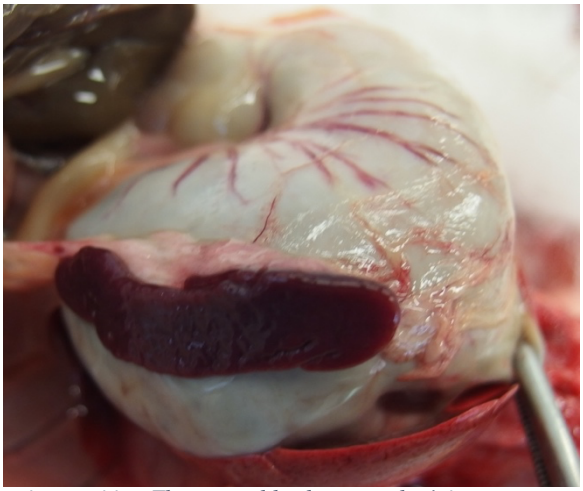

Spleen, rabbit. There is mild splenomegaly. (Photo courtesy of: Department of Veterinary Medicine, The Queen's Veterinary School Hospital, University of Cambridge. Cambridge CB3 0ES, UK. https://www.vet.cam.ac.uk)

areas contain moderate numbers of heterophils and small numbers of lymphocytes. In centrilobular regions there are small numbers of heterophils within sinusoids. In one section there is a focal grouping of portal areas mildly expanded by collagen bundles (fibrosis) with mild bile duct hyperplasia (this feature is not present in all sections submitted).

Contributor's morphologic diagnosis:

1. Hepatocellular necrosis, periportal and midzonal, acute, diffuse, marked; liver, with
    a. Hepatitis, portal, heterophilic, acute, diffuse, moderate.
2. Portal fibrosis, chronic, focal, mild; liver with
    a. Bile duct hyperplasia, chronic, focal, mild.

Contributor's comment:

The gross findings described in this case correlate with gross findings for RHDV-2 reported in the literature including a pale, friable liver with enhanced lobular pattern, splenomegaly, and renal petechiae.[8] Gross findings may vary in severity and can include splenomegaly, petechial or ecchymotic hemorrhages in various organs, hemorrhage within body cavities and/or pulmonary hemorrhage and oedema.[1] The most significant microscopic finding reported for RHDV-2 is periportal hepatocellular necrosis with varying degrees of severity, from scattered, individual necrosis of periportal hepatocytes to more diffuse, zonal necrosis, as in this case. Other reported findings include heterophilic infiltration of portal areas and hepatic parenchyma.[8] Calcification of individual hepatocytes has not

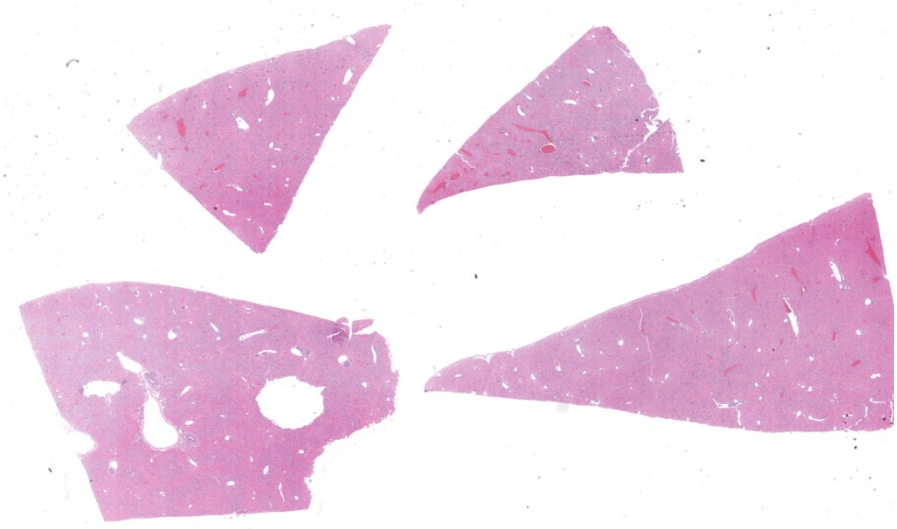

Liver, rabbit. Periportal and midzonal necrosis of hepatocytes and surviving centrilobular hepatocytes results in a retiform pattern of eosinophilia (necrosis) and basophilia (viable hepatocytes).

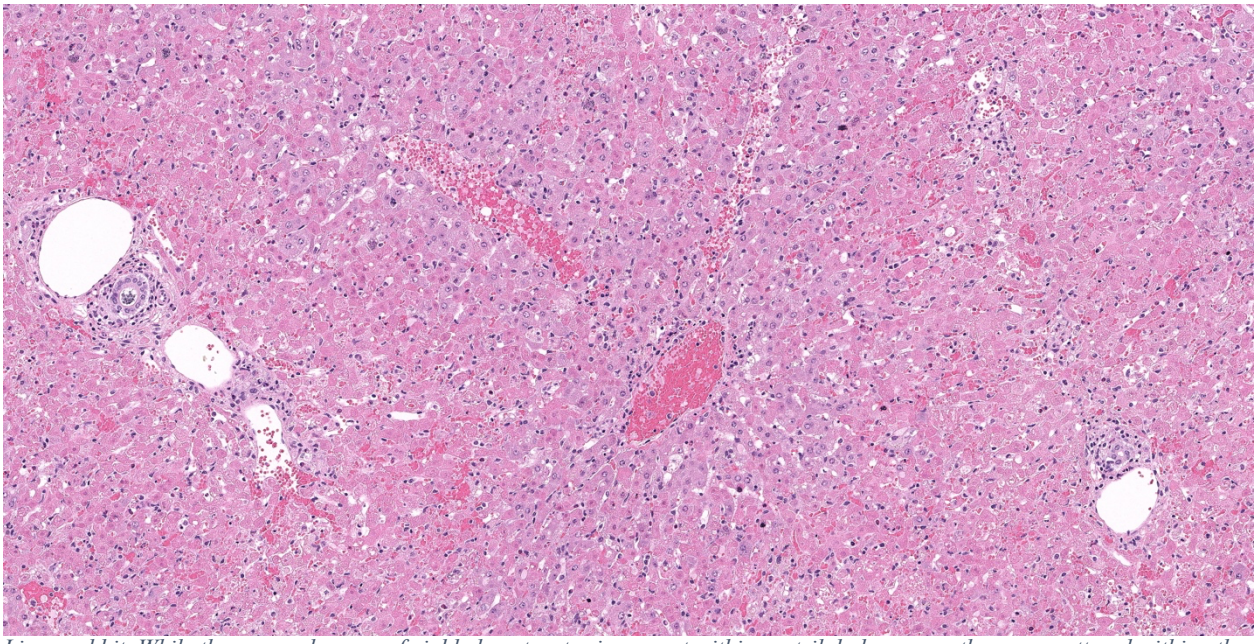

Liver, rabbit. While the preponderance of viable hepatocytes is present within centrilobular areas, they are scattered within other regions of the lobules. Some necrotic/apoptotic hepatocytes (and Kupffer) cells are mineralized. (HE, 400X)

been reported in experimentally infected rabbits, although it has been reported in hares infected with European brown hare syndrome virus, a *Caliciviridae* closely related to RHDV. In these cases, the cytoplasmic granules corresponded ultrastructurally to mitochondrial calcification.[6] The focal portal fibrosis and bile duct hyperplasia is considered most likely to be an unrelated finding in this case. The diagnosis can be confirmed by detection of RHDV-2 RNA in tissues or body fluids, ideally within fresh liver or spleen. RT-PCR is a rapid, highly sensitive method of detection that is readily available in Europe.[5]

RHDV is a member of the Lagovirus genus in the *Caliciviridae* family, along with European brown hare syndrome virus. *Caliciviridae* are positive sense, single stranded RNA viruses enclosed in an icosahedral capsid. A new, distinct variant of RHDV, named RHDV-2 or *Lagovirus europaeus*/GI.2/RHDV2/b, was first detected in France in 2010[7] and subsequently in other mainland European countries and Great Britain.[10] By 2018 it had been detected in Africa, Oceana, western Asia, and North America affecting both domestic and wild rabbits.[9] While some of the earliest RHDV-2 strains in France were reported to have a mortality rate of 20-30%, more recent strains in Europe and Australia have mortality rates of 70-100%.[4] Unlike RHDV-1, kittens are highly susceptible to RHDV-2.[8] Transmission can be direct through contact with infected rabbits shedding virus in secretions or via a fecal-oral route. Indirect transmission can occur via contaminated fomites such as food, bedding, clothing or equipment or via mammalian, avian or blood-feeding insect vectors.[1] The RHDV virus binds host-cell histo-blood group antigens (HBGA) on the surface of upper respiratory tract or gastrointestinal tract epithelial cells. After

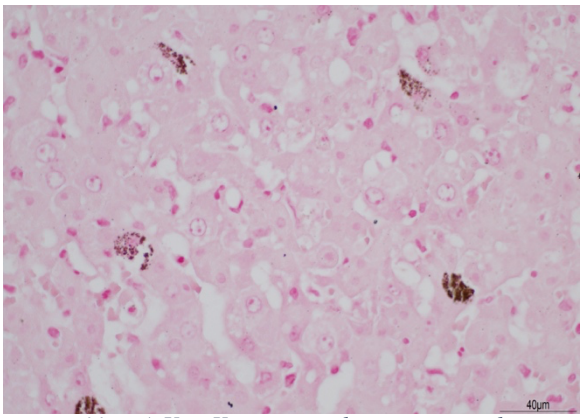

Liver, rabbit. A Von Kossa stain demonstrates calcium as dark black granules on the surface on hepatocytes and Kupffer cells. (Photo courtesy of: Department of Veterinary Medicine, The Queen's Veterinary School Hospital, University of Cambridge. Cambridge CB3 0ES, UK. https://www.vet.cam.ac.uk)

internalization and desencapsidation the positive sense RNA viral genome proceeds to translation and replication. The virus targets the liver rapidly following infection and replicates within hepatocyte cytoplasm. Structural protein VP10, which is translated from open reading frame 2 (ORF2), promotes apoptosis and so contributes to the cytopathic effects of the virus.[1]

Contributing Institution:
Department of Veterinary Medicine,
The Queen's Veterinary School Hospital,
University of Cambridge.
Cambridge CB3 0ES, UK.
https://www.vet.cam.ac.uk

JPC diagnosis:
Liver: Necrosis, periportal and midzonal, diffuse, with rare hepatocellular mineralization.

JPC comment:
Rabbit hemorrhagic disease virus (RHDV) remains an important pathogen in rabbit populations, causing mass mortality events from either natural infection, or as a method of population control. Domesticated rabbits were introduced to Australia in the 19th century, and the first reported feral population of rabbits was in Tasmania in 1827. They reached areas of mainland Australia (New South Wales, Queensland) by 1886 and spread to their present-day range by 1910. As an introduced/invasive species to Australia, they are prolific procreators, compete with native wildlife for food resources, and prevent some plant regrowth by eating seeds and seedlings. Rabbits are implicated as a potential cause of extinction of several small grown-dwelling mammals, the local decimation of two plant species, and a threat to populations of small mammals, plants, and some seabirds.[2]

The Commonwealth Government (federal Australian Government) uses a multipronged approach to reduce the population of rabbits, including biologic pathogens, chemicals, and mechanical interventions. Chemical methods include poisoning with sodium fluoroacetate, chloropicrin, and carbon monoxide, with physical destruction of habitat and warrens also a component of control. While one biologic method of control is the Myxoma virus, they also regularly release one strain of RHDV-2. The rabbit populations have developed resistance, and research into releasing new strains is under way.[2]

A recent case of RHDV in a German zoo affected the population of captive mountain hares. Previous research has shown that experimental infection with GI.1 RHDV in European brown hares induces antibody production but does not result in clinical disease. Hare populations experience differing extent of disease, with many species reporting significant pathology and mortality associated with GI.2 RHDV-2 strains. Sequencing of the isolated virus confirmed a previously sequenced strain of GI.2, suggesting the importance of cross-species transmission of this virus in endemic areas.[3]

The basophilic stippling seen multifocally on viable hepatocytes in this slide stained positively for both Von Kossa (indicating mineral) and a Perl's iron stain and was ultimately diagnosed as ferrugination. The cause of this is unclear and a similar change was seen in the 2019 WSC in a case of a dog with widespread necrosis due to CAV-1.

References:

1. Abrantes J van der Loo W, Le Pendu, Esteves PJ. Rabbit haemorrhagic disease (RHD) and rabbit haemorrhagic disease virus (RHDV): a review. *Vet Res.* 2012;43(1):12-31.
2. Australian Government, Department of Sustainability, Environment, Water, Population and Communities. Feral European Rabbit (*Oryctolagus cuniculus*). 2011. https://www.environment.gov.au/system/files/resources/7ba1c152-7eba-4dc0-a635-2a2c17bcd794/files/rabbit.pdf. Accessed on 19 Oct 2020.
3. Buehler M, Jesse ST, Kueck H, et al. Lagovirus europeus GI.2 (rabbit hemorrhagic disease virus 2) infection in captive mountain hares (*Lepus timidus*) in Germany. *BMC Veterinary Research*. 2020;16:166.
4. Capucci L, Cavadini P, Schiavitto M, Lombardi G, Lavazza A. Increased pathogenicity in rabbit haemorrhagic disease virus type 2 (RHDV2). *Vet Rec.* 2017;180(17):426-427.
5. Duarte DM, Carvalho CL, Barros SC, et al. A real time Taqman RT-PCR for the detection

of rabbit hemorrhagic disease virus 2 (RHDV2). *J Virol Methods*. 2015;219:90–95.
6. Gavier-Widén D. Morphologic and Immunohistochemical Characterization of the Hepatic Lesions Associated with European Brown Hare Syndrome. *Vet Pathol.* 1994;31(3):327–334.
7. Le Gall-Reculé G, Zwingelstein F, Boucher S, et al. Detection of a new variant of rabbit haemorrhagic disease virus in France. *Vet Rec.* 2011;168(5):137–138.
8. Neimanis A, Larsson Pettersson U, Huang N, Gavier-Widén D, Strive T. Elucidation of the pathology and tissue distribution of *Lagovirus europaeus* GI.2/RHDV2 (rabbit haemorrhagic disease virus 2) in young and adult rabbits (*Oryctolagus cuniculus*). *Vet Res*. 2018;49(1):46-60.
9. Rouco C, Aguayo-Adán JA, Santoro S, Abrantes J, Delibes-Mateos M. Worldwide rapid spread of the novel rabbit haemorrhagic disease virus (GI.2/RHDV2/b). *Transbound Emerg Dis*. 2019;doi:10.1111/tbed.13189.
10. Westcott DG & Choudhury B. Rabbit haemorrhagic disease virus 2-like variant in Great Britain. *Vet Rec.* 2015;176(3):74-76.

CASE 2: 18-2108 (4117382-00)

Signalment:
Fourteen-year-old, black Percheron gelding (*Equus ferus caballus*)

History:
A previously healthy gelding that received routine veterinary and dental care 6 days prior to death. The gelding was hitched to a cart at an event when it suddenly refused to go forward and within seconds, dropped to the ground. After a few spasms, it was declared dead.

Gross Pathology:
The horse was in good physical condition, well-fleshed, but not obese. The myocardium of the right atrium, right ventricle, and interventricular septum were streaked with numerous, well demarcated, white striae that extended transmurally from epicardium to endocardium. Adjacent papillary muscles were variably streaked as well. The left ventricular wall

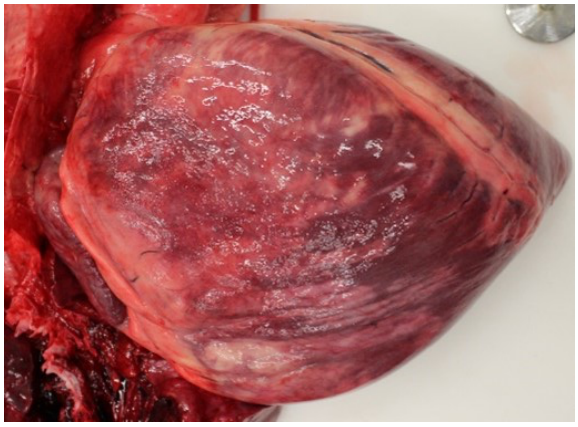

Heart, horse. Large coalescing white streaks are present within the right ventricular myocardium. (Photo courtesy of: University of Connecticut, Connecticut Veterinary Medical Diagnostic Laboratory, Department of Pathobiology and Veterinary Science College of Agriculture, Health and Natural Resources, http://patho.uconn.edu)

contained variably sized (1-5 cm diameter), irregularly round, well demarcated, bright white foci. Additionally, the epiglottis, larynx, and tracheal mucosa were speckled with petechial hemorrhages and the lungs were markedly congested.

Laboratory results:
None.

Microscopic description:
HEART (right ventricular wall and interventricular septum): Up to 75% of the right ventricular myocardium is replaced by adipose tissue, proliferating fibroblasts, and collagenous connective tissue. The tunica of most myocardial arteries is thickened up to 3-4 times normal by a circumferential proliferation of smooth muscle cells and collagen fibers (hypertrophy and hyperplasia), and most are surrounded by variable amounts of collagen fibers. Numerous myocardial fibers are swollen and pale, often fibrillar or fragmented, frequently contain 1-2 large vacuoles, and some exhibit significant variation of the diameter (atrophy). In another less affected section (interventricular septum), there is mild multifocal loss of myofibers and replacement by fibrous connective tissue. Randomly scattered throughout both sections, myofibers contain glassy, pale basophilic, PAS-positive, sarcoplasmic material that expands and sometimes completely replaces the fiber.

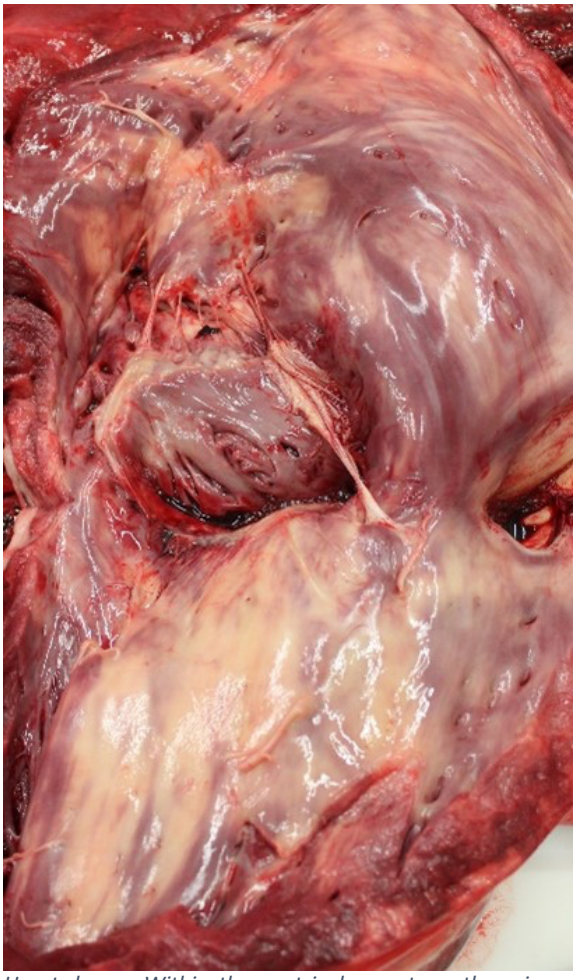

Heart, horse. Within the ventricular septum, there is an extensive patch of fibrofatty infiltration. (Photo courtesy of: University of Connecticut, Connecticut Veterinary Medical Diagnostic Laboratory, Department of Pathobiology and Veterinary Science College of Agriculture, Health and Natural Resources, http://patho.uconn.edu)

SKELETAL MUSCLE (tissue not submitted): Up to 60% of the myofibers display the following changes; diffuse pallor, loss of cross striations, sarcoplasmic swelling, and internalized nuclei. These fibers are infiltrated by few to moderate numbers of lymphocytes, macrophages, and plasma cells. There is accumulation of PAS-positive sarcolemmnal vacuoles in degenerative and normal myofibers. These vacuoles form coalescing aggregates that can completely replace the myofiber.

Contributor's morphologic diagnosis:
HEART (right ventricular free wall and interventricular septum):

1. moderate to marked arterial medial hyperplasia and hypertrophy;
2. mild to marked extensive myofiber degeneration and loss, with interstitial fibrosis and fatty infiltration;
3. mild to moderate myofiber accumulation of PAS-positive material

Contributor's comment:
Polysaccharide storage myopathy (PSSM) in this Percheron gelding was confirmed by the identification of PAS-positive intrasarcoplasmic polysaccharide inclusions in multiple muscles and the heart.[4,10] The distribution of changes in the heart were consistent with chronic vascular disease with secondary cardiac remodeling as opposed to a sequel of myocarditis.[3] Presumably, myocardial degeneration, fatty change, and interstitial fibrosis, can impact the conduction system by blocking conducting pathways or forming ectopic foci of electrical excitation, resulting in sudden death.[3,8]

PSSM is a condition caused by an autosomal dominant, gain of function, missense mutation (R309H) in the glycogen synthase gene (GYS1).[7,8] GYS1, a ubiquitously expressed enzyme, has a high expression in tissues with increased glycogen demand and metabolism, such as skeletal and cardiac muscle.[7] While the pathogenesis is unclear, mutation in this enzyme results in accumulation of amylase-resistant alpha-crystalline polysaccharide.[4,8,10,13] In humans, a similar mutation in GYS1, can present with a cardiac phenotype with cardiac failure or

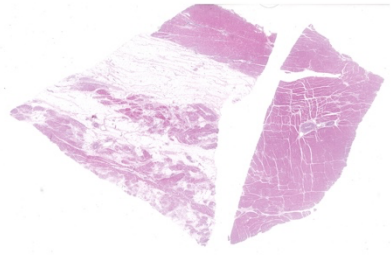

Heart, horse. Two sections of myocardium are submitted for examination. In one section, the myocardium is extensively replaced by fat. (HE, 200X)

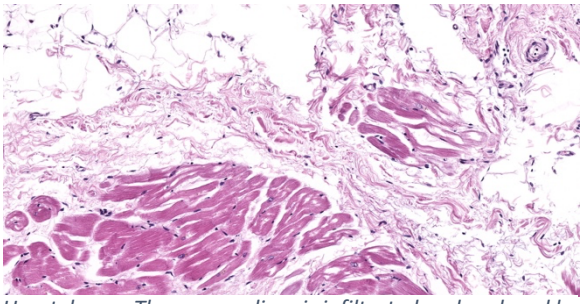

Heart, horse. The myocardium is infiltrated and replaced by abundant well-differentiated adipocytes and fibrous connective tissue and entrapped cardiomyocytes demonstrate marked atrophy, but few other features of degeneration. However, numerous cardiomyocytes exhibit one or occasional more clear sarcoplasmic vacuoles. (HE, 200X)

dysrhythmias.[11] In horses, PSSM has a wide range of clinical presentations, from no clinical signs, to muscle pain, shivers, ataxia, severe weakness, exertional rhabdomyolysis, and recumbency.[8,10,13] Diagnostic criteria for PSSM is controversial, but common criteria include the presence of PAS-positive +/- amylase resistant sarcoplasmic inclusions, subsarcolemmal glycogen aggregates, central cytoplasmic glycogen aggregates, in the presence of myopathic changes.[4,13]

Causes of myocardial disease in horses include viral infections (Equine Influenza, Equine Viral Arteritis, Equine Infectious Anemia, Equine Herpes Virus 1), bacterial infections (*Streptococcus* spp, *Staphylococcus* spp, *Salmonella* spp, *Clostridium* spp), parasitic infection (*Strongylus vulgaris, Onchocerca* spp), ingestion of cardiotoxic plants (*Nerium oleander*, *Digitalis purpurea, Convallaria majalis, Rhododendron* spp), ingestion of ionophore antibiotics (monensin, lasalocid, salinomycin), cantharidin toxicosis (blister beetle), and vitamin E/selenium deficiency.[3,10] The etiology of chronic myositis and myocardial fibrosis in horses remains unknown, although any cause of myocarditis can result in myocardial scarring.[3,10] This horse had no known history of disease or toxin exposure. Additionally, to our knowledge, there have been no confirmed reports of conduction defects in horses with PSSM and few reports of polysaccharide inclusions in the myocardium.[8,15] Percherons, Belgians, and other Draft horses have a particularly high prevalence of both type I polysaccharide storage myopathy and involvement of cardiac muscle.[8,13,15] In mice, glycogen storage myopathy and an over-expression of AMP-activated protein kinase results in conduction defects. The proposed mechanism of cardiac failure in humans and mice is distortion of the annulus fibrosis by vacuole-laden ventricular myocytes which allows an electrical impulse to by-pass the atrioventricular node and independently activate the ventricular myocardium.[1]

Contributing Institution:
University of Connecticut
Connecticut Veterinary Medical Diagnostic Laboratory
Department of Pathobiology and Veterinary Science College of Agriculture, Health and Natural Resources
http://patho.uconn.edu

JPC diagnosis:
Heart, myocardium: Myofiber cytoplasmic glycogen-like inclusions, numerous, with multifocal to coalescing myofiber degeneration and loss, with marked fibrofatty infiltration.

JPC comment:
This case generated lively discussion about the fibrofatty replacement of myocytes, and whether this was likely a result of the EPSSM, or potentially a different process. Previous investigations in horses with PSSM have found sporadic fatty infiltration and replacement of myocytes, with a particularly severe case found in a homozygous horse.[2] However, the clinical history of sudden collapse and death, the fibrofatty infiltration of the right ventricle, right atrium, and interventricular septum may also be consistent with arrhythmogenic right ventricular

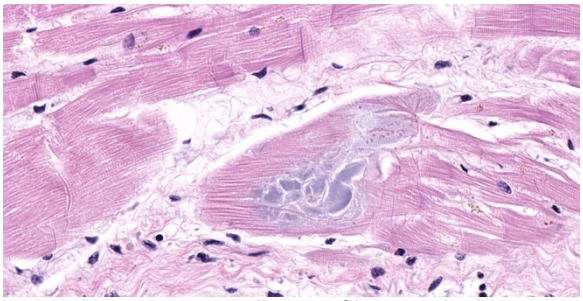

Heart, horse. Occasionally, myofibers in both sections contain rhomboidal to amorphous (shown here) accumulations of grey polysaccharides. (HE, 400X)

cardiomyopathy (ARVC). Reported cases have had patchy to diffuse fibrofatty infiltration and replacement of myocytes, few islands of adipose tissue within a loose collagenous stroma, with vacuolated and isolated or disrupted Purkinje fibers.[5,9]

Glycogen synthase (GS) is covalently regulated at nine phosphorylation sites which can be modified by various kinases. The kinases with the most significant contribution to decreased GS activity are glycogen synthase kinase 3β (GSK3β) and AMP-activated protein kinase (AMPK). Phosphorylation at four specific sites depress the enzyme activity than much more than the other five sites. Horses with homozygous mutant alleles had higher GS expression than wild types, and also had increased G6P-independent activity. As increased phosphorylation reduces GS activity, the elevation of GS activity remains despite increased phosphorylation of GS.[6]

Additional research examined the mitochondrial function of affected myocytes using high resolution respirometry (HRR), which has been used to detect mitochondrial dysfunction in humans. Certain mitochondrial dysfunctions have been associated with glycogen storage disease (GSD) in humans, such as GSD type II (Pompe disease), and GSD V (McArdle disease). While only a small group of affected horses was examined, there was a decrease in oxidative phosphorylation and electron transfer capacities in PSSM horses, with no substrate limitations evident. Different muscles examined (*gluteus medius*, *triceps brachii*) had different histopathologic appearances and levels of mitochondrial dysfunction, proposed to be due to different compositions and use of the muscle groups.[12]

PSSM that is due to GYS1 mutation has been categorized as PSSM type 1, and disproportionately affects Quarter horses, European-derived draught breeds, and related stock breeds. However, there remains a large population of cases of PSSM that are not correlated with GYS1 mutation, more often Warmblood and Arabian horses, and has been defined as PSSM type 2. A recently available genetic test for PSSM type 2 examines single nucleotide polymorphism (SNP) variants in the genes myotilin (*MYOT*), filamin C (*FLNC*) myozenin (*MYOZ3*). Unfortunately, in independent testing, there is no statistically significant correlation between gene status and diagnosis of PSSM type 2.[14]

References:

1. Arad M, Moskowitz IP, Patel VV, et al. Transgenic miceoverexpressing mutant PRKAG2 define the cause of Wolff-Parkinson-White syndrome in glycogen storage cardiomyopathy. *Circulation.* 2003; 107:2850–2856.
2. Barrey E, Mucher E, Jeansoule N, et al. Gene expression profiling in equine polysaccharide storage myopathy revealed inflammation, glycogenesis inhibition, hypoxia and mitochondrial dysfunctions. *BMC Veterinary Research*. 2009;5:29.
3. Buergelt, Claus D. Equine Cardiovascular Pathology: an Overview. *Animal Health Research Reviews*, 2003; 4 (2): 109–129.
4. Firshman, A. M, et al. Comparison of Histopathologic Criteria and Skeletal Muscle Fixation Techniques for the Diagnosis of Polysaccharide Storage Myopathy in Horses. *Veterinary Pathology*. 2006; 43 (3): 257–269.
5. Freel KM, Morrison LR, Thompson H, Else RW. Arrhythmogenic right ventricular cardiomyopathy as a cause of unexpected cardiac death in two horses. *Veterinary Record.* 2010; 166:718-722.
6. Maile CA, Hingst JR, Mahalingan KK, et al. A highly prevalent equine glycogen storage disease is explained by constitutive activation of a mutant glycogen synthase. *Biochimica et Biophysica Acta*. 2016;1861(1):3388-3398.
7. McCue ME, Valberg SJ, Miller MB, et al. Glycogen synthase (GYS1) mutation causes a novel skeletal muscle glycogenosis. *Genomics*. 2008; 91:458–466.
8. Naylor, et al. Evaluation of Cardiac Phenotype in Horses with Type 1 Polysaccharide Storage Myopathy. *Journal of Veterinary Internal Medicine*. 2012; 26(6): 1464–1469.
9. Raftery AG, Garcia NC, Thompson H, Sutton DGM. Arrhythmogenic right ventricular cardiomyopathy secondary to adipose infiltration as a cause of episodic collapse in a horse. *Irish Veterinary Journal*. 2015;68:24.

10. Robinson WF, Robinson NA. Cardiovascular system. In: Maxie MG, ed. *Jubb, Kennedy, and Palmer's Pathology of Domestic Animals*. 6th ed. Vol. 3. Philadelphia, PA: Elsevier, 2016:12–14.
11. Soliman OI, van der Beek NA, van Doorn PA, et al. Cardiac involvement in adults with Pompe disease. *J Intern Med*. 2008; 264:333–339.
12. Tosi I, Art T, Cassart D, et al. Altered mitochondrial oxidative phosphorylation capacity in horses suffering from polysaccharide storage myopathy. *Journal of Bioenergetics and Biomembranes*. 2018;50:379-390.
13. Valentine, B. A, and B. J Cooper. Incidence of Polysaccharide Storage Myopathy: Necropsy Study of 225 Horses. *Veterinary Pathology*. 2005; 42(6); 823–827.
14. Valberg SJ, Finno CJ, Henry ML, et al. Commercial genetic testing for type 2 polysaccharide storage myopathy and myofibrillar myopathy does not correspond to a histopathologic diagnosis. *Equine Veterinary Journal.* 2020. https://doi.org/10.1111/evj.13345
15. Valentine, B. A., et al.Severe Polysaccharide Storage Myopathy in Belgian and Percheron Draught Horses. *Equine Veterinary Journal*. 1997; 29(3); 220–225.

CASE 3: T18-6702 (4152981-00)

Signalment:
1-year-old, Female, German shepherd, dog (*Canis familiaris*)

History:
The dog exhibited neurological signs, had difficulty in walking, was not able to swallow, was drooling saliva, and was apparently blind. Encephalitis was suspected on clinical grounds; the dog was euthanized, and the carcass was submitted for necropsy.

Gross Pathology:
On external examination, it was noted that the dog was found in a poor body condition. Upon opening the carcass, the submandibular lymph nodes were moderately to markedly enlarged. Extensive multinodular mass that involved mediastinal lymph nodes and adjacent left side lungs was present in the thorax. The mass apparently compressed the adjacent thoracic esophageal segment. A small area of creamy exudate consistent with inspissated pus was present on cut surface, while grayish white surface was evident in the remaining nodular growths when cut. Right side lung was adhered to the diaphragm and the parietal pleura by moderate fibrous growth. Intestines had loose contents. There was a focal brainstem hemorrhage adjacent to cerebellum. There was no other grossly visible lesion.

Laboratory results:
Brain was negative for rabies.

Microscopic description:
Multifocal to focally extensive areas of granulomatous inflammation that contained abundant fungal yeasts admixed with macrophages were observed in the meninges of the brain. The fungal yeasts measured about 4-20 microns in diameter occasionally exhibiting a narrow-based budding and had thick transparent capsule consistent with Cryptococcus species. Similar lesions with abundant fungal yeasts were observed in multiple tissues and organs (slides not included) including skin, lungs, and lymph nodes.

Contributor's morphologic diagnosis:
Multifocal, moderate to severe granulomatous meningitis with intralesional fungal yeasts consistent with Cryptococcus species. There was granulomatous pneumonia, pleuritic, lymphadenitis and dermatitis (slides not

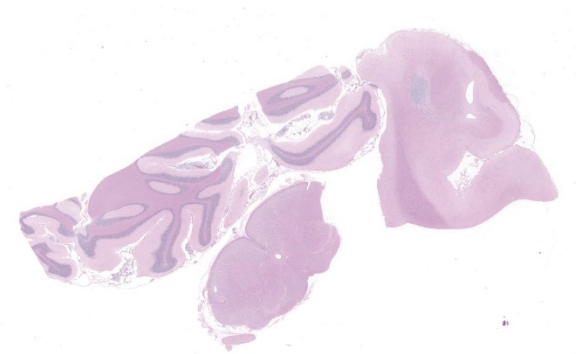

Brain, dog. Sections of cerebrum, cerebellum, and brainstem are submitted for examination. (HE, 5X)

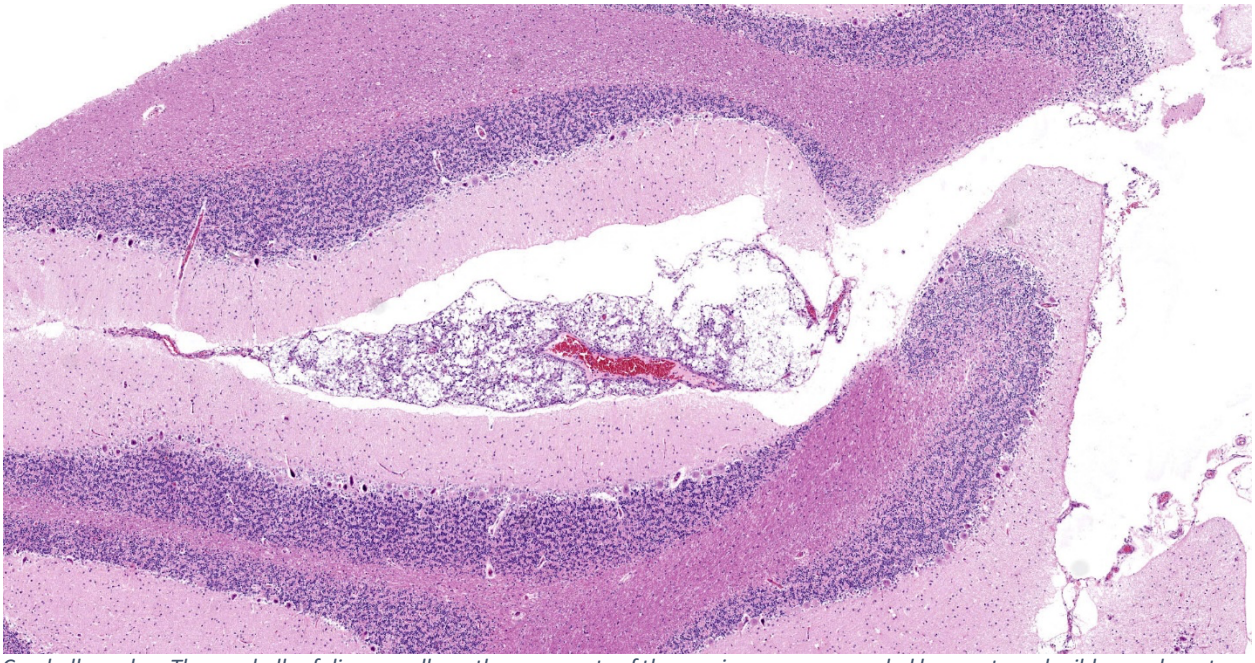

Cerebellum, dog. The cerebellar folia, as well as other segments of the meninges, are expanded by yeasts and mild granulomatous inflammation. (HE, 60X)

included) with intralesional similar fungal yeasts consistent with disseminated cryptococcosis.

Contributor's comment:
Multifocal to focally extensive severe, granulomatous to pyogranulomatous meningitis, dermatitis, pneumonia, pleuritis, lymphadenitis, peri-neuritis (optic nerve), splenitis, and with intralesional abundant fungal yeasts consistent with disseminated cryptococcosis were observed on microscopic examination.

Cryptococcosis is a mycosis caused by yeasts of genus Cryptococcus. The genus Cryptococcus can be divided into 2 groups: the pathogenic complex of *Cryptococcus neoformans* and *Cryptococcus gattii*, and the "less pathogenic" saprophytes, *Cryptococcus laurentii*, *Cryptococcus magnus*, and *Cryptococcus albidus* (although the species in the saprophyte group have been recently identified as pathogens in non-canine domestic animals).[2] Mainly *C. neoformans* and *C. gattii* affect humans and animals. The yeasts are widely distributed in the environment and are typically associated with avian droppings and decaying wood.[3] Cryptococcosis is distributed particularly in North America (Southern California, Western British Columbia), and on the east coast of Australia, while it has remained sporadic to date in Europe.[1]

Cryptococcosis caused by *Cryptococcus neoformans* and *C. gattii* is now being considered an important infectious disease both in humans and animals. The organism is isolated from environmental sources such as plant materials and avian excreta, where the fungus finds its ecological niche to reproduce, disperse and become the possible source of infections for the host.[7] Various domestic and wild mammals may be infected with Cryptococcus, including cats, dogs, ferrets, horses, camelids, goats, sheep, cattle, dolphins, koalas and other marsupials. Cryptococcosis most often occurs by inhalation of fungal yeasts in suspension in the air. The organisms lodge in the nasal, paranasal, and pulmonary tissues before spreading more widely by blood or direct extension[1,3] into other tissues including the central nervous system and cutaneous tissues.

Cryptococcus neoformans, an opportunistic fungus, is a commonly incriminated species in cryptococcosis. Immunosuppressive or debilitating diseases and iatrogenic

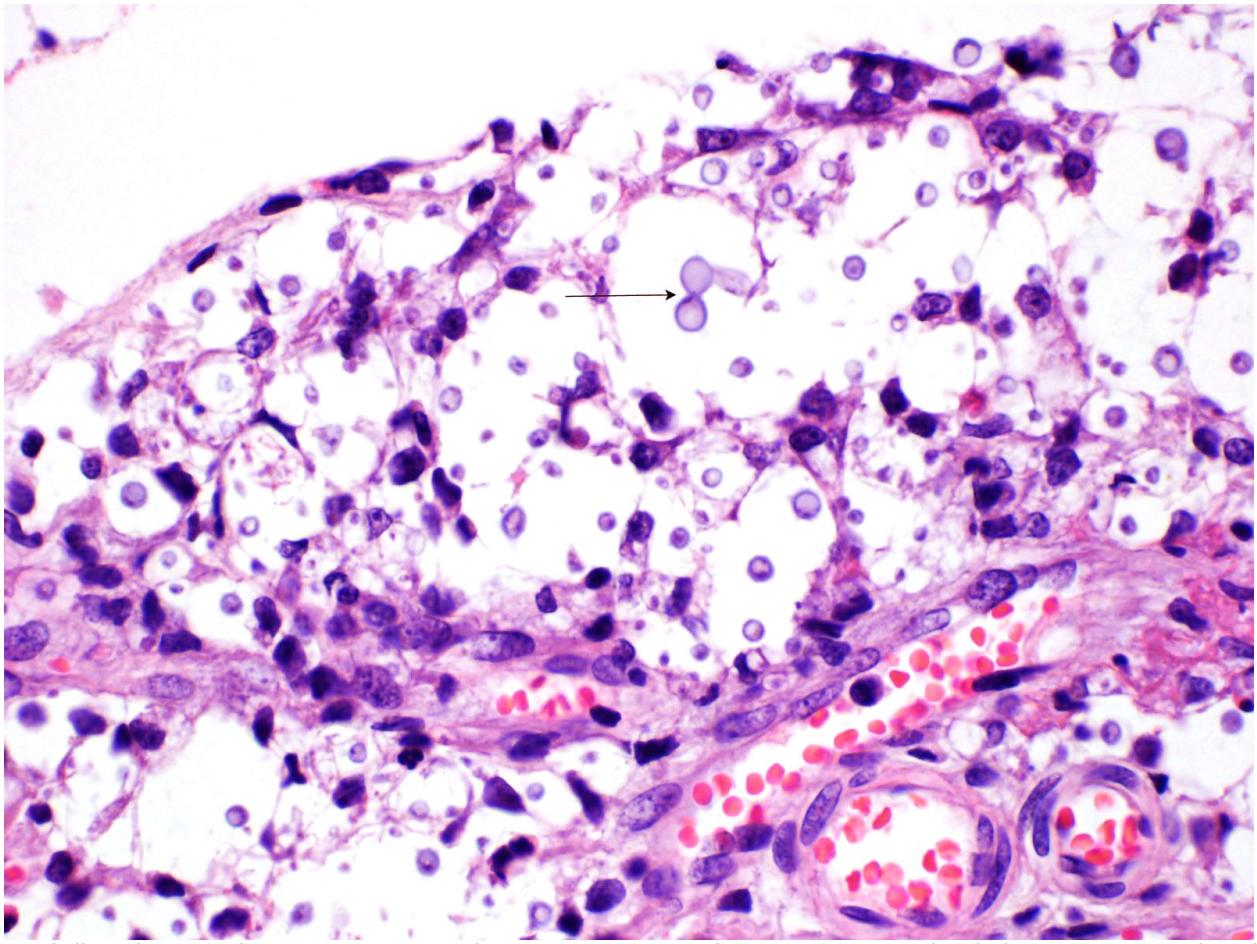

Cerebellum, dog. Granulomatous meningitis with numerous Cryptococcal yeasts organisms with a thick transparent capsule and narrow-based budding (arrow). (Photo courtesy of: The University of Georgia, College of Veterinary Medicine, Department of Pathology, Tifton Veterinary Diagnostic and Investigational Laboratory, 43 Brighton Rd, Tifton, GA 31793, USA) (HE, 400X)

glucocorticoids or cytotoxic chemotherapy is usually associated with cryptococcosis. There also was moderate demodicosis in the sections of skin in the dog in this report. *C. neoformans* presents a wide distribution in the environment and is associated mainly with avian droppings and decaying wood and most infections are linked to immunocompromised conditions. Similar to human cryptococcosis, the most likely route of infection in dogs and cats is inhalation of basidiospores or desiccated yeast cells during environmental exposure. Therefore, the nasal cavity is potentially the initial site of infection. Consequently, the most frequent clinical signs observed in veterinary medicine are associated with the upper and lower respiratory tracts.[3] The incidence of cryptococcosis is lower in dogs than in cats. Cryptococcosis particularly affects dogs under 6 years old. American Cocker Spaniels, Great Danes, Doberman Pinschers, and German Shepherds appear to be overrepresented.[1] The majority of canine cryptococcosis cases are reported as neurologic, disseminated, or nasal infections. A boxer dog is reported to suffer from primary alimentary cryptococcosis without dissemination.[9]

Cases of cryptococcosis in dogs are characterized mainly by the presentation of a systemic dissemination of infection, resulting in life threatening illness. The disease may occur in any age, but the majority of the cases have been reported in dogs younger than 6 years of age.[7] Clinical signs may vary depending on the severity of lesions and affected organs or tissues. In dogs, disseminated disease is frequent, severe, and often involves atypical sites. Major systems affected include central nervous system, eyes,

urinary system, and nasal cavity. Lytic bone lesions can cause lameness. Mild to moderate non-regenerative anemia, leukocytosis, monocytosis, and eosinophilia are common findings. There can be hematogenous spread, particularly to the central nervous system with incubation times 2-13 months or longer.[2]

Diagnosis of the infection can be made by routine culture techniques, histopathology and validated serological tests in all of medical mycology.[8] Cytological examination is also a good technique to detect *Cryptococcus* spp. in clinical cases[3] although a negative result in the cytology does not rule out the possibility of an infection.[7] *Cryptococcus* spp. could also be identified on fecal examination.[9]

Cryptococcosis remains hard to treat in dogs and cats, with the treatment consisting of the use of systemic antifungals that can be used as monotherapy or in combination. There is, however, not a clearly established protocol.[1] The entire resection of masses is reported to be an important step for the treatment of some patients. Long-term association of flucytosine, itraconazole and amphotericin B on postoperative care resulted in no relapse. The use of fluconazole and terbinafine were also associated with success in the treatment of gastrointestinal cryptococcosis.[3.] Canine abdominal cryptococcosis is reported to be successfully treated with a triazole therapy alone.[9]

The prognosis for cryptococcosis is poor and directly correlates with the extent and the magnitude of the disease at the time of the diagnosis. Implementation of an adequate treatment and rigorous monitoring can, however, quite substantially increase the chances of survival. Despite establishment of a suitable antifungal treatment, the prognosis remains poor.[1] The presence of clinical signs of CNS disease has been shown to be a significant predictor of mortality.[2]

Contributing Institution:
The University of Georgia
College of Veterinary Medicine
Department of Pathology
Tifton Veterinary Diagnostic and Investigational Laboratory
43 Brighton Rd, Tifton, GA 31793, USA

JPC diagnosis:

1. Cerebrum, cerebellum, spinal cord: Meningoencephalitis, granulomatous, multifocal to coalescing, moderate with numerous extracellular and intrahistiocytic encapsulated yeasts.
2. Cerebrum, presumptive pyriform lobe: Glioma.

JPC comment:
Cryptococcus neoformans is well summarized by the contributor. A polysaccharide capsule is the most critical virulence factor for this pathogen. The ability to form the capsule is dependent on local factors and host signals, such as the presence of glucose, iron, CO_2, which are sensed by the G-protein coupled receptor Gpr4 and the cyclic AMP/protein kinase A (cAMP/PKA) pathway. The cAMP/PKA pathway also coordinates capsule production through the regulation of transcription factors, the ubiquitin proteasome system, and the iron regulator Cir1. Some virulence factors, such as melanin, are also regulated through the cAMP/PKA pathway, while others (proteases, urease, phospholipase, and superoxide dismutase) are regulated in other ways.[5]

Acapsular *Cryptococcus* spp yeasts have been reported in animal infections occasionally. The variants without a capsule are typically less virulent than those with a functional capsule. A basic component of the fungal cell wall is α-1,3-glucan encoded by the *AGS1* gene, which critical for the correct capsule-cell wall attachment. Variants with disruptions to the *AGS1* gene (*ags1*Δ strain) are characterized by yeasts that are functionally alive, but without any capsule on the cell wall surface, despite the correct presence of capsule components in sufficient quantities.[4]

While not regularly reported in veterinary literature, *Cryptococcus* spp can also form cells of varying size. While the normal yeast size is approximately 4-6 μm in diameter, titan cells are larger than 12 μm in diameter, and sometimes

larger than 100 µm in diameter. Like many other regulatory mechanisms in this genus, titan cell production is also regulated by the cAMP/PKA pathway.[4,5] On the other size of normal, *Cryptococcus* spp also has the ability to make micro cells that are usually 2-4 µm in diameter and may be adapted for growth in macrophages.[4]

Interestingly, a few slides (and the distributed scanned slide) for this case contain a focus of glial proliferation within what appears to be a section of pyriform lobe. Our opinion on this focus, which lacked inflammatory cells as well as yeasts and is based solely on morphology is that it represents a small glioma. Dr. Jey Koehler of Auburn University agreed in consult. Olig2, GFAP, IBA1, CD3, and PAX5 were performed, but this focus was unfortunately not present in the submitted unstained slides.

References:

1. Barbry J-B, Poinsard AS, Gomes E, et al. Cryptococcosis with ocular and central nervous system involvement in a 3-year-old dog. *Clin Case Rep*. 2019; 7:2349–2354.
2. Block K, Battig J. Cryptococcal Maxillary Osteomyelitis and Osteonecrosis in a 18-Month-Old Dog. *J Vet Dent*, 2017; 34 (2):76-85.
3. de Abreu DPB. Machado CH. Makita MT. et al. Intestinal Lesion in a Dog Due to *Cryptococcus gattii* Type VGII and Review of Published Cases of Canine Gastrointestinal Cryptococcosis. Mycopathologia. 2017; 182:597–602.
4. Frank KM, McAdam AJ. Infectious Diseases. In: Kumar V, Abbas AK, Aster JC, eds. *Robbins and Cotran Pathologic Basis of Disease*, 10th Ed. Philadelphia, PA:Elsevier. 2020;385.
5. Garcia-Rubio R, de Oliveira HC, Rivera J, Trevijano-Contador N. The Fungal Cell Wall: *Candida*, *Cryptococcus*, and *Aspergillus* Species. *Frontiers in Microbiology*. 2020;10:2993.
6. Mayer FL, Kronstad JW. *Cryptococcus neoformans*. *Trends in Microbiology*. 2020;28(2):163-164.
7. Pérez F, Avila O, Vélez N, Escandón P. Cryptococcosis in Dogs: A Case Report in a Labrador retriever in Bogotá, Colombia. *Med Mycol Open Access*. 2015, 1:4. doi: 10.21767/2471-8521.100004
8. Perfect JR, Bicanic T. Cryptococcosis Diagnosis and Treatment: What Do We Know Now. Fungal Genet Biol. 2015; 78: 49–54.
9. Tangeman L, Davignon D, Patel R, et al. Abdominal Cryptococcosis in Two Dogs: Diagnosis and Medical Management. *J Am Anim Hosp Assoc.* 51(2):107-13.

CASE 4: A19-1839 (4152506-00)

Signalment:
17 years, female, military macaw, *Ara militaris,* macaw

History:
Regurgitation and wasting.

Gross Pathology:
The 780 g macaw was wasted with severe pectoral muscle atrophy and no appreciable coelomic adipose tissue. The proventriculus (not submitted to WSC) was distended with feed and approximately 8 cm in length. The wall of the proventriculus was markedly thin. The proventriculus was adhered to nearby tissues by strands of fibrin.

The ventriculus (submitted tissue) was flaccid with severe, diffuse thinning of the muscular wall.

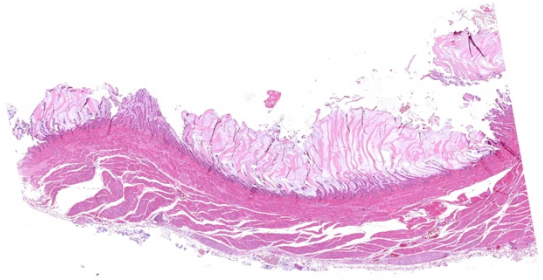

Ventriculus, macaw: A single cross section of the ventriculus is presented for examination. There is diffuse thinning of the ventricular smooth muscle. (HE, 5X)

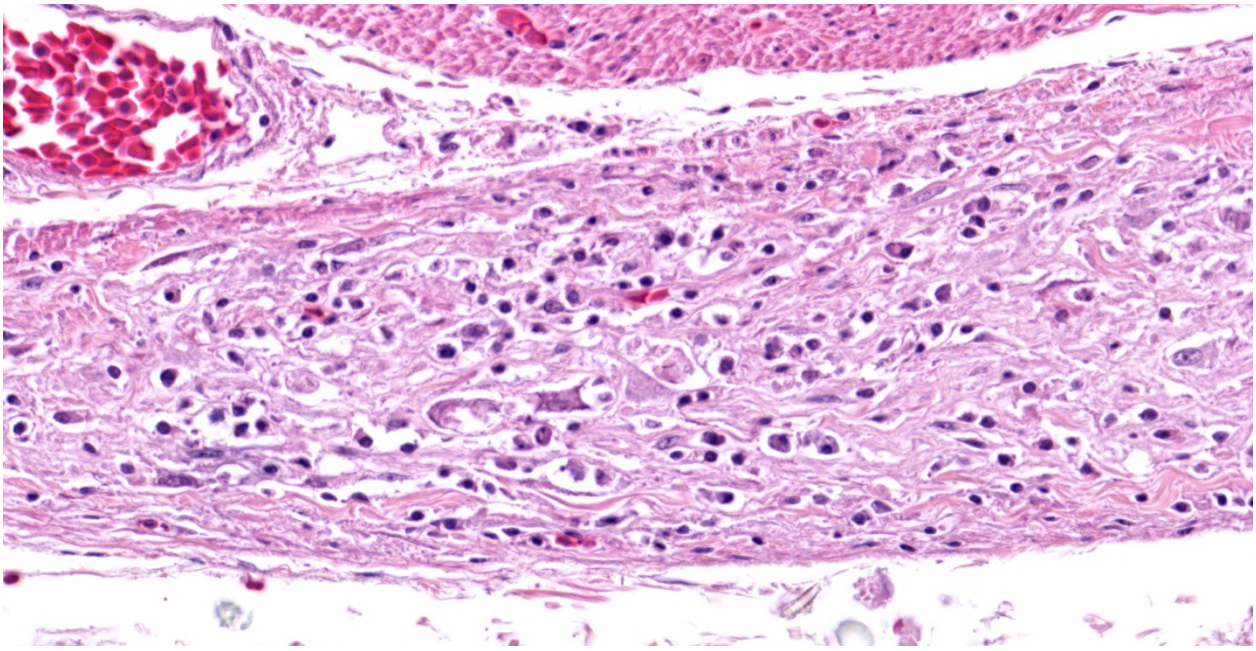

Ventriculus macaw: Moderate numbers of lymphocytes infiltrates autonomic nerves, separating nerve fibers. Nerve cell bodies are dark and contracted, and there is mild neural edema. (HE, 500X)

Laboratory results:
Aerobic culture of the liver and culture of liver and gastrointestinal tract for Salmonella were negative.

No parasites were observed on fecal flotation.

Microscopic description:
In the section of ventriculus, numerous lymphocytes and plasma cells are in nerve fiber bundles and ganglia of the autonomic plexi. Smooth muscle bundles of the tunica muscularis are atrophied with variable lymphocytic inflammation. Axons and neuronal cell bodies are degenerated or lost with a relative increase in endoneurial fibrous tissue. Similar histologic lesions were in the crop and proventriculus (not submitted).

Contributor's morphologic diagnosis:
Lymphoplasmacytic ganglioneuritis with muscular atrophy, ventriculus

Contributor's comment:
The lymphoplasmacytic inflammation of gastrointestinal autonomic plexi prompted a diagnosis of proventricular dilatation disease (PDD). Coupled with the gross lesions of proventricular dilation, the autonomic ganglioneuritis is considered diagnostic of PDD. Immunohistochemistry and PCR can be used for confirmation, using brain, especially thalamus or hind brain, or other tissues.[8] Dilation of the proventriculus (distension by feed), the major gross lesion at autopsy, is attributed to the ganglioneuritis in the autonomic nervous system, especially that of the gastrointestinal tract.[8] Other lesions can include encephalomyelitis, peripheral neuritis, myocarditis, and adrenalitis.

A viral cause had long been suspected for PDD, and in 2008, separate research teams identified novel avian bornaviral strains by DNA sequencing and PCR of the brain and other tissues from parrots with PDD.[3,5] Originally named avian bornavirus, the etiologic agent is now called parrot bornavirus. Fecal-oral transmission has been proposed as the natural route of infection; however, oculonasal or oral inoculation failed to establish persistent infection or disease in cockatiels.[2] Intramuscular (pectoral) inoculation with parrot bornavirus-2 consistently resulted in infection, with virus appearing first in the caudal segments of the spinal cord with rostral spread to the brain.[6] The gastrointestinal autonomic nervous system was not evaluated in that study, but in natural infection, gastrointestinal signs, attributable to ganglioneuritis of the autonomic

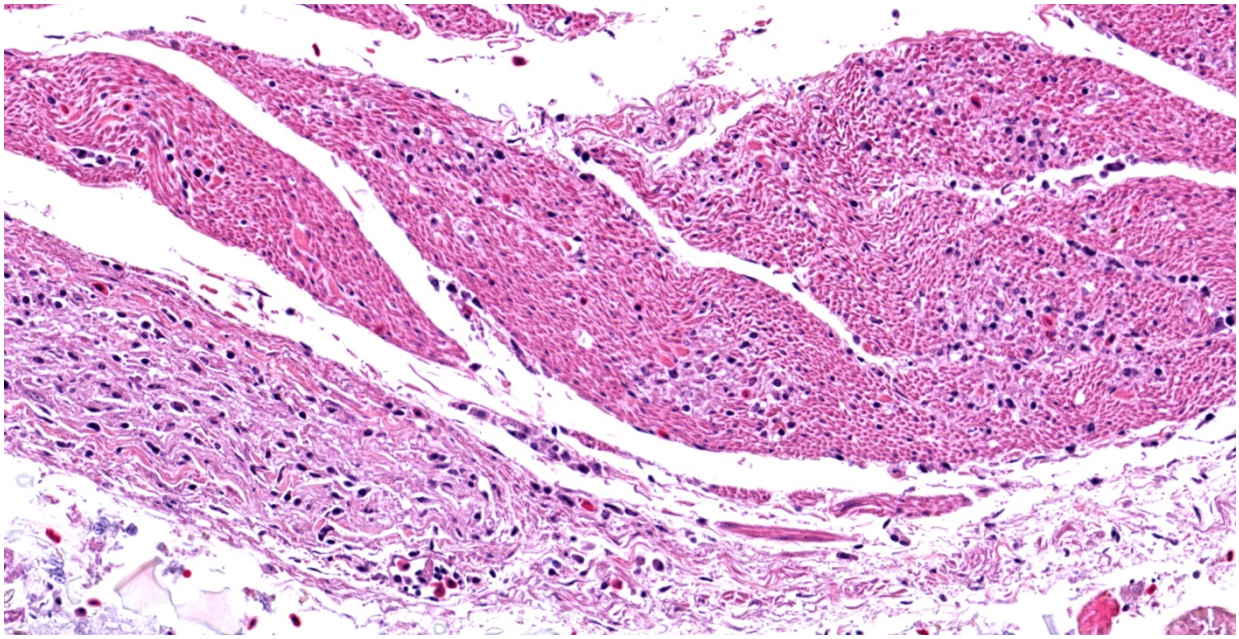

Ventriculus, macaw: In addition to nerve fibers, infiltration of smooth muscle bundles by lymphocytes and plasma cells results in focal myofiber necrosis and atrophy. (HE, 500X)

nervous system, typically precede the development of signs of encephalomyelitis.

Clinical signs of PDD[3] include regurgitation and weight loss, which were reported in this macaw. Infected birds can carry the bornavirus asymptomatically and shed it intermittently in feces and urates. Clinical signs develop as the bird mounts an immune response to the virus. The lymphoplasmacytic inflammation causes progressive destruction of peripheral nerves, ganglia, spinal cord, and brain. Disease progression can be slow or rapid.

Contributing Institution:
Purdue University
Animal Disease Diagnostic Laboratory: http://www.addl.purdue.edu/

Department of Comparative Pathobiology: https://vet.purdue.edu/cpb/

JPC diagnosis:
Ventriculus: Ganglioneuritis and leiomyositis, lymphoplasmacytic, multifocal, moderate, with neuronal necrosis and myofiber atrophy.

JPC comment:
Currently, there are 15 enumerated avian bornavirus (ABV) genotypes that make up six viral species, which include psittaciform bornavirus (PaBV) 1, 2, and 4[7], passeriform bornavirus-1, passeriform bornaavirus-2, and waterbird bornavirus 1. Within these species are often several strains specific to different host bird species. Shedding of the virus is intermittent, but PCR testing of urine, feces, and cloacal swaps are most likely to contain ABV RNA. However, a negative result does not rule out infection.[4]

There are a number of other conditions that may result in similar clinical signs as ABV, some of which include gastrointestinal parasites, tumors, papillomas, granulomas, foreign bodies, or heavy metal toxicity (particularly lead).[4]

If available, immunohistochemistry (IHC) is a useful modality to evaluate tissue for ABV infection. Anti-ABV antigen is most often located in the nucleus of affected cells, such as ganglia, brain, spinal cord, adrenal glands, pancreas, kidneys, anterior gastrointestinal tract, heart, testes, ovaries, and thyroid glands.[3,7] Investigation into lymphoplasmacytic infiltration of Purkinje fibers, epicardium, myocardium,

endocardium, and great vessels of naturally and experimentally infected birds with PaBV was closely associated with epicardial ganglioneuritis. In many cases, affected cells were immunolabeled with anti-PaBV antibodies.[1,7]

Avian bornaviruses share characteristics with their mammalian counterparts, including a well-established correlation between the onset of neurologic signs and the presence of CD3+ T lymphocytes in the brain. Beyond the lesions noted in the central nervous system, inflammatory infiltrates are most often composed of lymphocytes, macrophages, and variable numbers of plasma cells, suggesting an important link between clinical disease and the adaptive immune system. Avian bornavirus also appears to inhibit type 1 IFN signaling, as well as trim viral genomic 5'-phosphates to evade recognition by RIG-1 receptors. Current antiviral therapies are working to leverage these mechanisms.[7]

During case discussion, one pathologist experienced with avian pathology opined that the inflammation in smooth muscle in this case may not represent true leiomyositis per se, but inflammation extending along neuronal axons as they traverse the adjacent smooth muscle.

References:

1. de Araujo JL, Hameed SS, Tizard I, et al. Cardiac lesions of natural and experimental infection by parrot bornaviruses. *J Comp Path*. 2020;174:104-112.
2. Heckmann J, Enderlein D, Piepenbring AK, et al. Investigation of different infection routes of parrot bornavirus in cockatiels. *Avian Dis*. 2017;**61**:90-95.
3. Honkavuori KS, Shivaprasad HL, Williams BL, et al. Novel borna virus in psittacine birds with proventricular dilatation disease. *Emerg Infect Dis*. 2008;**14**(12):1883-1886.
4. Hoppes SM, Shivaprasa HL. Update on Avian Bornavirus and Proventricular Dilitation Disease. *Vet Clin Exot Anim*. 2020;23:337-351.
5. Kistler AL, Gancz A, Clubb S, et al. Recovery of divergent avian bornaviruses from cases of proventricular dilatation disease: identification of a candidate etiologic agent. *Virol J*. 2008;**5**:88-102.
6. Leal de Araujo J, Rodrigues-Hoffmann A, Giaretta PR, et al. Distribution of viral antigen and inflammatory lesions in the nervous system of cockatiels (*Nymphicus hollandicus*) experimentally infected with parrot bornavirus 2. *Vet Pathol.* 2019;**56**(1):106-117.
7. Nobach D, Muller J, Tappe D, Herden C. Update on immunopathology of bornavirus infections in humans and animals. *Advances in Virus Research*. 2020;107:159-222.
8. Venâncio Donatti R, Resende M, Ferreira Junior FC, et al. Fatal proventricular dilatation disease in captive native psittacines in Brazil. *Avian Dis.* 2014;**58**:187-193.